Journal of Theoretical Biology 479 (2019) 1–13

Contents lists available at ScienceDirect

Journal of Theoretical Biology

journal homepage: www.elsevier.com/locate/jtb

Cyclic prey evolution with cannibalistic predators

Sami O. Lehtinen*, Stefan A.H. Geritz

Department of Mathematics and Statistics, University of Helsinki, FIN 00014, Finland

ARTICLE INFO

Article history:
Received 7 February 2019
Revised 19 June 2019
Accepted 28 June 2019
Available online 29 June 2019

Keywords:
Adaptive dynamics
Ecological bistability
Fold bifurcation of periodic orbits
Subcritical Hopf bifurcation
Supercritical Hopf bifurcation

ABSTRACT

We investigate the evolution of timidity in a prey species whose predator has cannibalistic tendencies. The ecological model is derived from individual-level processes, in which the prey seeks refuge after detecting a predator, and the predator cannibalises on the conspecific juveniles. Bifurcation analysis of the model reveals ecological bistability between equilibrium and periodic attractors. Using the framework of adaptive dynamics, we classify ten qualitatively different evolutionary scenarios induced by the ecological bistability. These scenarios include ecological attractor switching through catastrophic bifurcations, which can reverse the direction of evolution. We show that such reversals often result in evolutionary cycling of the level of timidity. In the absence of cannibalism, the model never exhibits ecological bistability nor evolutionary cycling. We conclude that cannibalistic predator behaviour can completely change both the ecological dynamics and the evolution of prey.

1. Introduction

Most prey species have strategies against predation, such as group defence, camouflage, and defensive armour. A simple yet common strategy is to avoid the predators by being timid, that is, to seek refuge after detecting a predator. Such timid behaviour has consequences for both the prey and the predator species. The prey benefits from a reduced risk of predation, but since foraging in refuge is typically unfeasible, timidity has a negative effect on the overall foraging effort. On the other hand, timid behaviour may also result in decreased prey availability for the predator. This prompts the predator to search for alternative prey or resort to cannibalism, as is common in many predator species. The literature provides a plethora of observed examples, ranging from fish and insects to birds and mammals (Fox, 1975; Polis, 1981). For instance, in the spider *Lycosa lugubris* cannibalism accounts to 85% of juvenile mortality (Edgar, 1969), while in the crow *Corvus corone* 75% of the eggs are cannibalised (Yom-Tov, 1974). The evolution of timidity and cannibalism in the predator-prey context has been studied using several mathematical models (Matsuda and Abrams, 1994; Dercole and Rinaldi, 2002; Geritz and Gyllenberg, 2014; Vitale and Kisdi, 2018). These include a study that considered the evolutionary consequences of an alternative prey (Vitale and Kisdi, 2018). However, previous studies that address cannibalism neglect timidity, and vice versa. In this paper, we investigate the evolution of timidity in a prey species whose predator has cannibalistic tendencies.

Evolution by natural selection is ultimately driven by interactions between individuals. These interactions form the basis for the ecological environment, which changes gradually over the course of evolution. To describe the direction in which phenotypic traits evolve, one needs to know the state of the ecological environment, that is, the ecological attractor. While most evolutionary models share the notion that the phenotypic traits uniquely determine the ecological attractor, real environments can have multiple stable attractors (Scheffer et al., 2001). Such ecological bistability has been found to cause abrupt switching between alternative ecological attractors (May, 1977) or catastrophic collapse of the ecosystem (Rietkerk et al., 2004). Thus, it is essential to derive the ecological model from the individual-level processes, so that every model parameter can be clearly interpreted in terms of the individual behaviour (Rueffler et al., 2006). By doing so, one can sensibly identify the underlying individual-level processes that induce ecological bistability, and investigate how ecological bistability affects long-term evolutionary outcomes.

In models that contain ecological bistability, a single phenotypic trait can correspond to multiple ecological attractors, in which the directions of evolution are possibly different. Consequently, the paths of evolution should be investigated separately for each ecological attractor, where the branches of the attractors are traced during the course of evolution. When the gradual evolutionary changes in the phenotypic traits are sufficiently small and mutations occur infrequently, the changes in the ecological attractors

* Corresponding author.
E-mail address: sami.lehtinen@helsinki.fi (S.O. Lehtinen).

https://doi.org/10.1016/j.jtbi.2019.06.025

are also relatively small. Hence abrupt switching between alternative attractors is rare, and occurs only when the branch of the ecological attractors which is being traced disappears (Geritz et al., 2002). When the ecological environment undergoes such attractor switching, the direction of evolution may change as well. If further such drastic ecological changes occur, the evolutionary path could return to the original state. In other words, phenotypic traits would cycle on the evolutionary timescale.

Evolutionary cycling can be driven by many different mechanisms (Khibnik and Kondrashov, 1997; Kisdi et al., 2001). Various instances of evolutionary cycles are known in models of diverse nature, such as predator-prey systems (Dieckmann et al., 1995; Abrams and Matsuda, 1997; Law et al., 1997), multispecies coevolution (Khibnik and Kondrashov, 1997; Hui et al., 2018), and cooperative games (Hauert et al., 2002). Although evolution is typically considerably slower than ecological dynamics, in some instances cyclic evolution has been observed empirically (Decaestecker et al., 2007). All these studies share the same underlying mechanism of genetically driven cycles. Evolutionary cycling can also be driven by recurrent branching and extinction of cannibalistic predators (Kisdi et al., 2001; Dercole, 2003). However, ecogenetically driven cycles involving ecological attractor switching is present in fewer studies (Doebeli and Ruxton, 1997; Khibnik and Kondrashov, 1997; Dercole et al., 2002). These studies have ignored individual-level processes in the model derivation. Although these models produce intriguing outcomes, the lack of clear interpretation in terms of individual behaviour raises the question whether such outcomes are feasible in nature.

Several models have been proposed to investigate the evolution of timidity in the context of predator-prey dynamics. In an early study, Matsuda and Abrams (1994) considered a model with ecological bistability and a fixed predator population size, and found that the evolution of foraging effort can drive the prey species into extinction. Unfortunately, the model by Matsuda and Abrams lacked the derivation from individual-level processes. Later, Geritz and Gyllenberg (2014) enhanced ecological realism by deriving the model from individual-level processes, and assumed that also the predator population changes in the ecological dynamics. In particular, Geritz and Gyllenberg considered a prey that seeks refuge only after detecting a predator individual. The evolutionary analysis revealed that periodic predator-prey population attractors were necessary for timidity to be favourable by natural selection, while ecological bistability and evolutionary suicide were absent. In a more recent study, Vitale and Kisdi (2018) extended the model of Matsuda and Abrams (1994) by introducing an alternative prey that acts as the main resource for the predator. Vitale and Kisdi showed that in this extended model, evolutionary suicide of the focal prey can occur, similar to Matsuda and Abrams (1994).

The organisation of the paper is as follows. In Section 2 we derive a predator-prey model from individual-level processes with timid prey in the spirit of Geritz and Gyllenberg (2012,2014), but now also with cannibalistic predators. Then, in Section 3 we establish some analytical results concerning the existence and uniqueness of an interior equilibrium, and its stability properties. We also apply numerical bifurcation analysis, which reveals ecological bistability between equilibrium and periodic attractors. Next, in Section 4 the evolution of the timidity of the prey is analysed using the framework of adaptive dynamics (Geritz et al., 1998). We classify ten qualitatively different evolutionary scenarios, in which ecological bistability plays a central role. These include abrupt switching between the ecological attractors that may reverse the direction of evolution. We show that such reversals can result in evolutionary cycling of the level of timidity. Finally, in Section 5 we discuss the role of individual behaviour in both ecological bistability and evolutionary cycling. Throughout the paper, we rely on numerical examples that are easy to visualise. Frequently used symbols are found in Table 1.

Table 1
List of model parameters.

Prey parameters	
Symbol	Description
b	rate of moving to refuge
τ	mean sojourn time in refuge
μ	natural death rate
G	birth rate
Predator parameters	
Symbol	Description
α	rate of cannibalism
β	rate of prey capture
h	handling time per captured prey
γ	conversion factor of prey capture
λ	conversion factor of cannibalism
T	maturation time
δ	adult death rate
σ	juvenile death rate

2. Derivation of the ecological model

Consider an ecological environment consisting of a single prey species whose predator has cannibalistic tendencies. The predators are divided into adults and juveniles, in which the juveniles are the victims of cannibalism, and only the adults predate on the common prey. Within the prey species, many different prey types may coexist that are assumed to differ only in their level of timidity. Here, timidity is understood as a behavioural trait, which describes the readiness to seek and remain in refuge after detecting a predator individual. The prey in refuge are protected from predation, while their foraging has halted. As in Geritz and Gyllenberg (2012,2014), we assume that the prey detects a predator individual and moves to a refuge at the rate b, and τ is the mean sojourn time in the refuge. Although the handling predators are harmless to the prey, they are unable to distinguish between searching and handling predators. However, since the juvenile predators are typically considerably smaller than the conspecific adults, we have reason to assume that the prey react only to the adult individuals. Throughout this paper, 'predator' without a specification always refers to an adult individual, as only the adults feed on the prey.

Thus, we divide each prey population x_i with the parameter values b_i and τ_i into foragers x_i^F and hiders x_i^H,

$$x_i = x_i^F + x_i^H. \tag{1}$$

Both foraging and hiding prey have the same natural death rate μ, which is independent of the prey and the predator populations. The foraging prey compete for some common resource, such as territory or breeding sites, so that their birth rate is limited by the total population of foraging prey. To make this pattern explicit, we assume that the per capita birth rate $G(\sum_j x_j^F)$ is monotonically decreasing, and assume the existence of x_0 such that $G(x_0) = \mu$. Therefore, in the absence of the predators, the prey populations attain the equilibrium state x_0, which is the carrying capacity of prey-only dynamics. Examples of mechanistic derivations of the per capita birth rate G based on competition for breeding sites or food are found in Appendix C of Geritz and Gyllenberg (2014).

As for the predator, we assume that a searching predator captures prey at the rate β, and the average handling time per captured prey is h. For each prey capture, the predators produce juveniles with the average conversion factor γ, and the juveniles have the mean maturation time T. The natural death rates of the adults and the juveniles are δ and σ, respectively. The conspecific juve-

niles have the population z, and the adult population y is divided into searchers y^S and handlers y^H,

$$y = y^S + y^H. \tag{2}$$

To extend the model of Geritz and Gyllenberg (2014), we assume that the adult predators cannibalise on the conspecific juveniles at the rate α, where cannibalism has the conversion factor λ. To keep the model simple, we assume that the handling time of cannibalism is negligible. Biologically, this assumption implies that the victims of cannibalism are smaller or otherwise easier to digest and kill than the typical prey. Indeed, many predator fish and insects cannibalise on eggs and post-hatching stages, in which the victims are unable to defend themselves and are considerably smaller than the cannibals (Fox, 1975; Polis, 1981). For example, the juveniles of Eurasian perch (*Perca fluviatilis*) feed on zooplankton, while the adults prey on fish, which includes cannibalism (Hjelm et al., 2000). Then, it stands to reason that the predator needs more rest after capturing a prey that can defend itself. Admittedly, in nature both the prey and the juveniles come in various sizes, hence a more realistic model could include a continuum of sizes that affect the handling times. However, analysis of such a size-structured model is beyond the scope and aim of this paper.

Since a total of five different individual states is present, the full ecological dynamics are described by a system of five ordinary differential equations (see Appendix A). To simplify the analysis, we reduce the number of equations by a separation of timescales. That is, we divide the full ecological dynamics into nested timescales by the occurrence of transitions between the individual states. These consist of short timescale for the transitions between foraging and hiding prey states, and between searching and handling predator states; intermediate timescale of juvenile predator birth and death; and long timescale of adult predator maturation and death, and prey birth and death. Admittedly, in nature the prey dynamics are likely occur also on the intermediate timescale, which could include their respective juvenile birth and death interactions. Here, the implicit assumption is that the juvenile prey are always in the refuge, so that their population dynamics are independent from the predators. Then, the prey birth term of our model corresponds to maturation of a juvenile prey, which now starts foraging.

To achieve the separation of timescales, we assume that the adult predator population is considerably smaller than the juvenile population, and that the prey are abundant. In addition, we make the following assumptions about the individual behaviour: the predators have a long maturation time, the prey are more likely to move to refuge than fall victim to predation, and cannibalism is commonplace for the predator. The precise technical details on how to achieve the timescale separation are found in Appendix A. There we also propose an alternative separation with only two timescales and different biological assumptions, but that nevertheless results in the same system of differential equations for the long timescale dynamics.

With the above assumptions, we obtain the following system of differential equations for the short timescale dynamics,

$$\dot{x}_i^F = -b_i x_i^F y + \frac{1}{\tau_i} x_i^H, \tag{3}$$

$$\dot{y}^S = -\beta y^S \sum_j x_j^F + \frac{1}{h} y^H. \tag{4}$$

Note that the population numbers x, y, and z are constants in this short timescale. The system of Eqs. (1)–(4) has unique quasi-steady state,

$$x_i^F = \frac{x_i}{1 + b_i \tau_i y}, \tag{5}$$

$$y^S = \frac{y}{1 + \beta h \sum_j x_j^F}. \tag{6}$$

Observe that the parameters b_i and τ_i are always found in the product $b_i\tau_i$, which describes the level of timidity of the prey (Geritz and Gyllenberg, 2014). Thus while timidity is a behavioural trait, it can be explicitly quantified by the product of two inheritable parameters. While two prey types with different parameter values may have the same level of timidity, we make no distinction between these prey types. For convenience, we treat this product as a single parameter, and write it as $b\tau_i$.

Next, assuming that the variables x_i^F and y^S have attained their respective quasi-steady states (5) and (6), we obtain the following differential equation for the intermediate timescale dynamics,

$$\dot{z} = \gamma \beta y^S \sum_j x_j^F + \lambda \alpha y^S z - \alpha y^S z - \sigma z. \tag{7}$$

A biological restriction on the efficiency of cannibalism is $\lambda < 1$, so that the number of juveniles lost to cannibalism is always greater than the new juveniles directly produced from cannibalism. This restriction essentially follows from the assumption that the victims of cannibalism are distinctly smaller (e.g. eggs), and fully cannibalistic predators are unable to sustain the population. However, when also larger conspecific individuals are being cannibalised, it is possible to sustain a population solely by means of cannibalism (Popova and Sytina, 1977; van den Bosch et al., 1988). Now, by using the Eqs. (5)–(7), we find that the juvenile predator population has unique quasi-steady state,

$$z = \frac{\gamma \beta y^S \sum_j x_j^F}{\sigma + (1-\lambda)\alpha y^S}. \tag{8}$$

Finally, assuming that the variable z has attained its quasi-steady state (8), we obtain the following system of differential equations for the long timescale dynamics,

$$\dot{x}_i = x_i^F G\Big(\sum_j x_j^F\Big) - \mu x_i - \beta x_i^F y^S, \tag{9}$$

$$\dot{y} = \frac{1}{T} z - \delta y, \tag{10}$$

where the variables x_i^F and y^S are given by (5) and (6), respectively. The functional response $F_i(x, y)$ of the predator for the prey type i is equal to the rate of prey capture $\beta x_i^F y^S$ divided by the total predator population y. As in Geritz and Gyllenberg (2014), the functional response is given by

$$F_i(x,y) = \frac{\beta x_i^F}{1 + \beta h \sum_j x_j^F} = \frac{\frac{\beta x_i}{1+b\tau_i y}}{1 + \beta h \sum_j \frac{x_j}{1+b\tau_j y}}, \tag{11}$$

which is the multi-prey version of the Beddington-DeAngelis functional response (Beddington, 1975; DeAngelis et al., 1975; Geritz and Gyllenberg, 2012). By rewriting the long timescale dynamics in terms of the functional response $F_i(x, y)$ and the quasi-steady states of y^S and z as given by (6) and (8), we obtain

$$\dot{x}_i = x_i^F G\Big(\sum_j x_j^F\Big) - \mu x_i - y F_i(x,y), \tag{12}$$

$$\dot{y} = \frac{\gamma(1 + \beta h \sum_j x_j^F) y \sum_j F_j(x,y)}{T(\sigma(1 + \beta h \sum_j x_j^F) + (1-\lambda)\alpha y)} - \delta y. \tag{13}$$

It is now clear that no constant parameter can describe the translation of each prey capture into the adult predator population. Although we assumed instantaneous production of juveniles, the transition to the adult population occurs only later after maturation. As the juveniles are subject to cannibalism, the rate of

maturation depends on the cannibalistic pressure they experience throughout their juvenile period. Moreover, at high prey populations the cannibalistic pressure is lower, due to a larger fraction of the predators being in the handling state. The rate of recruitment to the adult population is hence affected by both the prey and the predator populations, and is captured by the term

$$\frac{\gamma\left(1+\beta h\sum_j x_j^F\right)}{T\left(\sigma\left(1+\beta h\sum_j x_j^F\right)+(1-\lambda)\alpha y\right)}. \tag{14}$$

It would have been near impossible to arrive at a biologically sound interpretation of the term (14) without a mechanistic derivation.

In the limiting case when cannibalism is absent, $\alpha = 0$, the recruitment rate (14) is simply a constant $\gamma/(T\sigma)$. That is, without cannibalistic predators, the model is reduced into that of Geritz and Gyllenberg (2014), but the constant recruitment rate now has a slightly different interpretation. Furthermore, in the limiting case when both cannibalism and timidity are absent, $\alpha = b\tau = 0$, we recover the classical (Rosenzweig and MacArthur, 1963) model.

3. Ecological dynamics with a single prey type

When only a single prey type is present, the ecological dynamics described by (12) and (13) are given by

$$\dot{x} = x^F G\left(x^F\right) - \mu x - \frac{\beta x^F y}{1+\beta h x^F}, \tag{15}$$

$$\dot{y} = \frac{\gamma\beta x^F y}{T\left(\sigma\left(1+\beta h x^F\right)+(1-\lambda)\alpha y\right)} - \delta y, \tag{16}$$

where $x^F = x/(1+b\tau y)$. When the prey is at the predator-free equilibrium state x_0, an initially rare predator is viable if and only if the rate of prey capture and its conversion factor are sufficiently large,

$$\beta > \frac{\delta\sigma T}{x_0(\gamma - \delta\sigma h T)} \qquad \text{and} \qquad \gamma > \delta\sigma h T. \tag{17}$$

Note that the above condition is independent of the rate of cannibalism, α, or the level of timidity, $b\tau$.

Suppose that the conditions (17) are satisfied so that the predator can invade the ecological environment. Then, the ecological dynamics described by (15) and (16) have the following properties:

(i) Unique interior equilibrium $(\bar{x}, \bar{y})$ exists.
(ii) For every $b\tau$, at most one α exists where $(\bar{x}, \bar{y})$ undergoes a Hopf bifurcation.
(iii) For every α, at most one $b\tau$ exists where $(\bar{x}, \bar{y})$ undergoes a Hopf bifurcation.

The proofs are rather algebraic, and are found in Appendix B and Appendix C. Thus, if the interior equilibrium is unstable in the absence of both cannibalism and timidity, then increasing either cannibalism or timidity will eventually stabilise the equilibrium through a Hopf bifurcation. Afterwards, the equilibrium undergoes no further bifurcations.

The parameter values at which Hopf bifurcations occur were solved numerically. For the numerical analysis, we employed the following choice for the per capita birth rate G,

$$G(x^F) = \begin{cases} a - cx^F & \text{if} \quad 0 \le x^F < a/c, \\ 0 & \text{otherwise.} \end{cases} \tag{18}$$

This form follows when the prey is the consumer of a resource with a linear functional response, and where the resource grows logistically in the absence of the prey (Geritz and Gyllenberg, 2014). It is known that the Hopf bifurcation of the Rosenzweig and MacArthur (1963) model is always supercritical. Recall that for supercritical Hopf bifurcation, equilibrium and periodic solutions are arbitrarily near in the vicinity of the bifurcation, resulting in a continuous transition between these stable attractors. However, the numerical analysis revealed that in the model described by (15) and (16) both sub- and supercritical Hopf bifurcations can occur. If the equilibrium is stabilised through a subcritical Hopf, it generates an unstable periodic solution, but the periodic attractor is still present. Thus the ecological dynamics exhibit bistability between equilibrium and periodic attractors, where the regions of attraction are separated by the unstable periodic orbit. Furthermore, the two periodic solutions eventually collide and disappear through a fold bifurcation of periodic orbits (Kuznetsov, 1998). When a need arises to distinguish between different bifurcations, subindex and superindex H are used, respectively, for sub- and supercritical Hopf, and fold of periodic orbits is denoted by subindex F.

The numerical analysis was done using the *Mathematica*® software. Population sizes less than 10^{-16} were considered too small and no longer relevant for the analysis. To find periodic orbits, we numerically integrated (15) and (16) using an explicit Runge-Kutta method for *NDSolve*, and collected data of the population numbers at each point in time along the orbit. The convergence of the orbit was evaluated using a Poincaré section, which we implemented using the *EventLocator* method for *NDSolve*. The population numbers were collected until the distance between two consecutive equilibrium points of a Poincaré map was smaller than 10^{-5}, after which we discarded the transient data. Then, the periodic orbit is described by the data from the last iteration, and the period is the time-interval between the last two consecutive equilibrium points of the Poincaré map.

Stable periodic orbits were found using $(x, y) = (x_0, 0.001)$ as the initial value of the numerical integration, but in principle, any (x_0, y) with $y > 0$ works as well. This is because (x_0, y) must belong to the region of attraction, as $\dot{x} < 0$ for all (x_0, y). Unstable periodic orbits were found using the same method in reverse direction, and by choosing a non-equilibrium initial value from the interior of the stable periodic orbit. To find the value $b\tau_1$ at which two periodic orbits undergo a fold bifurcation, we first set an $b\tau$-interval in which the ecological dynamics corresponding to the left limit point contain bistability, while only the equilibrium attractor exists for the right limit point. Then, after checking the ecological dynamics at the middle point of the interval, we halved the interval so that it retains $b\tau_1$. We iterated the process until $b\tau_1$ was found with the accuracy of 10^{-5}.

Fig. 1 presents an example in which the ecological attractors undergo subcritical Hopf and fold bifurcations by increasing $b\tau$. When $b\tau = 0.4000$, the interior equilibrium is unstable and the predator-prey populations are at a periodic attractor. Then, at $b\tau_H = 0.4077$ the equilibrium stabilises through a subcritical Hopf bifurcation, after which the ecological dynamics exhibit bistability between equilibrium and periodic attractors, separated by an unstable periodic solution. By further increasing $b\tau$, the amplitude of the unstable solution also increases, whereas the amplitude of the stable solution decreases. At $b\tau_F = 0.4430$ these two periodic solutions collide and disappear through a fold bifurcation, after which the equilibrium is the only attractor and no further bifurcations occur.

Fig. 2 depicts which types of ecological attractors are present in the $(b\tau, \alpha)$-plane. The figures (a) and (b) correspond to two different rates of prey capture, β, demonstrating how fold bifurcation is unattainable when β is small. Fig. 2(a) illustrates that when the rate of prey capture is low, $\beta = 11$, the ecological dynamics behave similarly to the Rosenzweig and MacArthur (1963) model. That is, when $b\tau$ and α are sufficiently small, the ecological attractor is periodic and the interior equilibrium is unstable. By increasing ei-

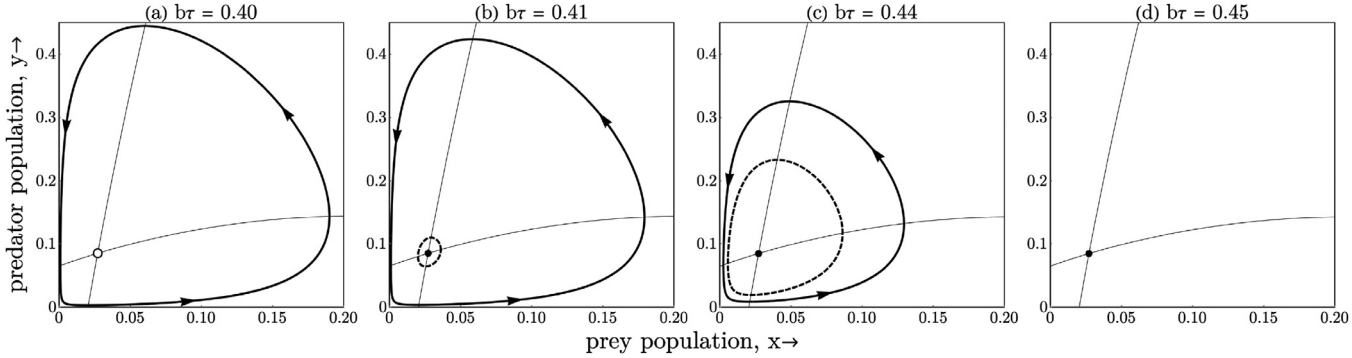

Fig. 1. Predator-prey ecological attractors for different levels of timidity. Thick lines: ecological attractors; Dashed lines: unstable periodic solution; Closed circles: Stable equilibrium; Open circles: Unstable equilibrium; Thin lines: predator-prey isoclines, where directional change is absent. In this figure, $c = 2$, $a = 2$, $\mu = 1$, $\gamma = 3$, $\lambda = 0.6$, $\delta = 1$, $h = 1$, $T = 1$, $\sigma = 0.7$, $\alpha = 6$, and $\beta = 15$.

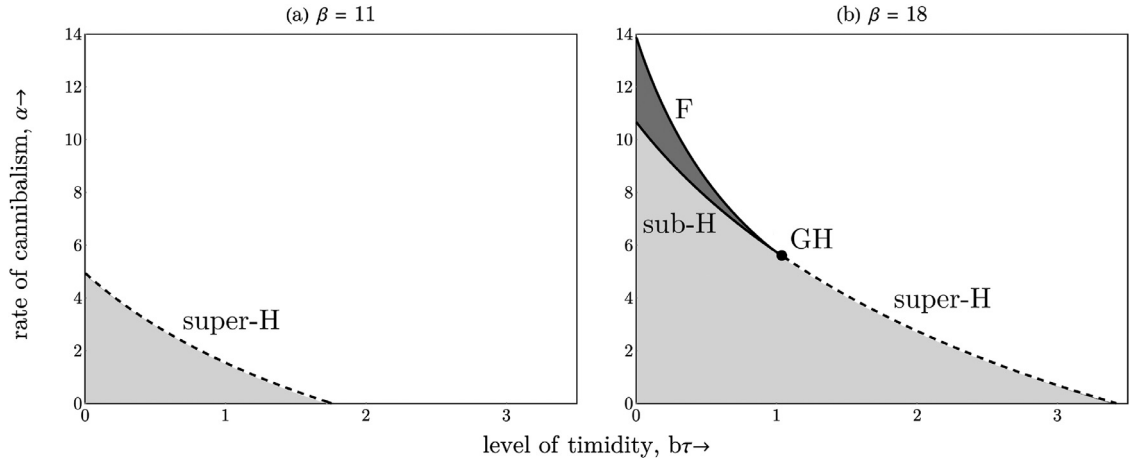

Fig. 2. Bifurcation diagrams for the ecological model in the $(b\tau, \alpha)$-plane. White: stable equilibrium; Light gray: periodic attractor; Dark gray: bistability between equilibrium and periodic attractors. The lines at which supercritical Hopf, subcritical Hopf, and fold bifurcations occur are denoted by, respectively, super-H, sub-H, and F. The generalised Hopf bifurcation is denoted by GH. In this figure, $c = 2$, $a = 2$, $\mu = 1$, $\gamma = 3$, $\lambda = 0.6$, $\delta = 1$, $h = 1$, $T = 1$, and $\sigma = 0.7$.

ther of these parameters stabilises the equilibrium through a supercritical Hopf bifurcation, after which the equilibrium is the only attractor and no further bifurcations occur.

Fig. 2(b) illustrates that when the rate of prey capture is large, $\beta = 18$, the ecological dynamics are qualitatively different from the previous example. When $b\tau$ and α are sufficiently small, the ecological attractor is periodic and the equilibrium is unstable. Then, increasing either of these parameters stabilises the equilibrium through a Hopf bifurcation, which can be either sub- or supercritical. Whenever the equilibrium is stabilised through a subcritical Hopf, the ecological dynamics exhibit bistability between equilibrium and periodic attractors. Then, further increasing either of these parameters causes a fold bifurcation. The generalised Hopf occurs when the bifurcation switches from being subcritical to supercritical, which in this example occurs at $b\tau = 1.2610$ and $\alpha = 4.8110$. That is, for $\alpha < 4.8110$, supercritical Hopf is the only possible bifurcation, whereas for $10.6756 > \alpha > 4.8110$, both subcritical Hopf and fold bifurcations are possible. For $13.7880 > \alpha > 10.6756$, Hopf bifurcation is no longer possible for any $b\tau$, but ecological bistability is still present when $b\tau = 0$ and fold bifurcation happens for some $b\tau_F > 0$. Finally, for $\alpha > 13.7880$ fold bifurcation is no longer possible, which disappears through the boundary $b\tau_F = 0$ when $\alpha = 13.7880$. That is, for $\alpha > 13.7880$ the interior equilibrium is the only attractor and no bifurcations happen for any $b\tau$. Thus, for the parameters in Fig. 2(b), ecological bistability is possible for $4.8110 < \alpha < 13.7880$, and for each fixed α in that interval, the bistability is present for a different set of $b\tau$ values.

In Fig. 3, we extend the above examples by letting both α and β vary. That is, for each combination of α and β, we investigate all possible bifurcations that occur by varying the level of timidity, $b\tau$. In this way, we find four regions of qualitatively different bifurcations, denoted A-D. The left panel of Fig. 3 shows a typical example of these four regions in the (α, β)-plane, and the right panels show examples of the bifurcations for some α and β belonging to each of these regions. For simplicity, in these examples only the prey population numbers are shown, and when periodic solutions exist, we plotted only the maximum prey population at such periodic solutions.

In bifurcation region A, the interior equilibrium is the only attractor for all $b\tau$, and bifurcations never occur. Moreover, the prey population at the equilibrium remains largely unchanged when $b\tau$ varies, which is visible in Fig. 3 when $\alpha = 10$ and $\beta = 7$.

In bifurcation region B, a periodic attractor exists at $b\tau = 0$, where the interior equilibrium is unstable. Then, increasing $b\tau$ stabilises the equilibrium through a supercritical Hopf bifurcation, after which periodic attractors are absent. For example, when $\alpha = 0$ and $\beta = 6$, the supercritical Hopf occurs at $b\tau^H = 0.6289$.

In bifurcation region C, the dynamical behaviour at $b\tau = 0$ is the same as in B. But now increasing $b\tau$ stabilises the interior equilibrium through a subcritical Hopf bifurcation, which generates ecological bistability between equilibrium and periodic attractors. Further increasing $b\tau$ causes a fold bifurcation, whereupon the equilibrium is the only attractor and no further bifurcations occur. For example, when $\alpha = 8$ and $\beta = 16$, the subcritical Hopf

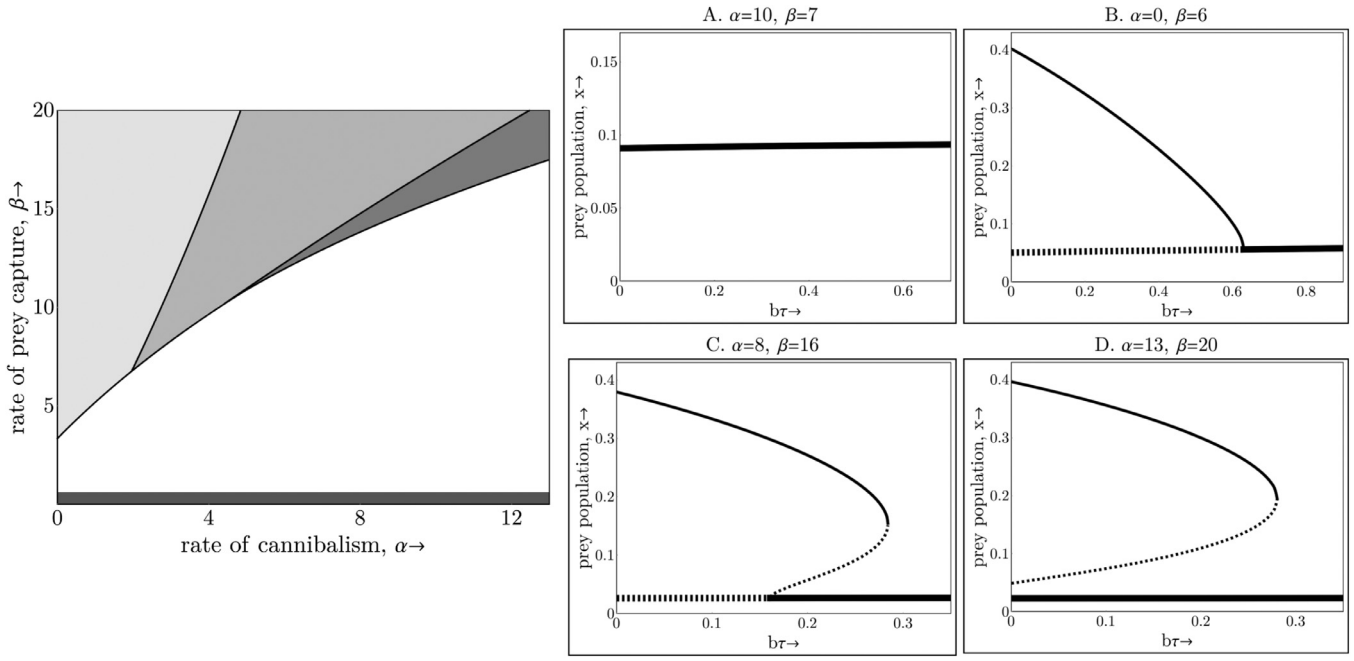

Fig. 3. The regions of qualitatively different bifurcations of $b\tau$ (*left*) and examples of the bifurcations corresponding to each region (*right*). In the panels on the right, thin curves represent the maximum of x along period orbits, while thick curves are the equilibrium numbers. Unstable solutions are shown using dashed curves. The parameters are the same as in Fig. 2.

and fold bifurcations occur at $b\tau_H = 0.1608$ and $b\tau_F = 0.2839$, respectively, and ecological bistability is present between these bifurcations.

In bifurcation region D, the interior equilibrium is stable for all $b\tau$, as in A. But now a periodic attractor also exists when $b\tau = 0$, implying the presence of ecological bistability for sufficiently small $b\tau$. For example, when $\alpha = 13$ and $\beta = 20$, fold bifurcation occurs at $b\tau_F = 0.2802$, after which ecological bistability is absent.

4. Evolution of timidity of the prey

In the previous section, we investigated bifurcations of the ecological dynamics by varying the parameters $b\tau$, α, and β. We found a wide range of values for which the ecological attractors disappear through subcritical Hopf and fold bifurcations. However, this analysis fails to provide any information whether evolution causes an ecological attractor to disappear, or how such an ecological change affects the course of evolution. To investigate these questions, we will now study the evolution of timidity of the prey. Recall that while timidity is a behavioural trait, it is characterised by the product of the two parameters b and τ that can be subject to natural selection. First, we write the ecological dynamics (12) for the prey type i in terms of the environment E,

$$\dot{x}_i = f(b\tau_i, E)x_i, \tag{19}$$

where $E = (E_1, E_2)$ is given by

$$\begin{aligned} E_1 &= y && \text{(predator density)},\\ E_2 &= \sum_j \frac{x_j}{1 + b\tau_j E_1} && \text{(foraging prey density)}, \end{aligned} \tag{20}$$

and where f is given by

$$f(b\tau_i, E) = \frac{1}{1 + b\tau_i E_1}\left(G(E_2) - \frac{\beta E_1}{1 + \beta h E_2}\right) - \mu. \tag{21}$$

Hence $f(b\tau_i, E)$ describes the per capita population growth rate for prey type i in environment E. Although the Eqs. (19)–(21) are identical to Geritz and Gyllenberg (2014), the dynamics of the environment E as described by (12) and (13) are different.

We study evolution using the framework of adaptive dynamics, the necessary preliminaries of which are found in Geritz et al. (1998). We assume that any mutant has only a small phenotypic effect on the resident trait. Moreover, mutations occur infrequently, so that the fate of the previous mutant has been established, and the ecological environment has attained an attractor by the time a new mutant appears. The resident environment determines the growth rate of a mutant population, while the environment is unaffected by an initially rare mutant. Whenever a mutant can invade a resident-generated environment, but invasion would be impossible if the roles were switched, the mutant replaces the resident. The Tube Theorem (Geritz et al., 2002) ensures that under these assumptions, through repeated invasion and replacement events the resident environment traces the same branch of ecological attractors as long as no catastrophic bifurcations occur, such as subcritical Hopf or fold bifurcation. However, if such a catastrophic bifurcation is encountered, the current branch of the ecological attractors disappears and the population either goes extinct or settles on an alternative attractor. In this paper, only the latter outcome can occur, as the prey or the predator species never go extinct by the evolution of timidity. This is clear since both the extinction equilibrium $(x, y) = (0, 0)$ and the prey-only equilibrium $(x, y) = (x_0, 0)$ are unstable for all levels of timidity.

Introduce a novel mutant prey with the level of timidity $b\tau_m$. That is, the mutant trait $b\tau_m$ differs from the resident through either b_m or τ_m, or through both of them, but it is essentially the product of these parameters that determines the mutant type. As before, we treat this product as a single parameter. The long-term invasion fitness of the mutant type $b\tau_m$ is the time average of the instantaneous population growth rate. In a periodic resident environment E set by a single resident type $b\tau$, the fitness of the mutant is described by

$$r_E(b\tau_m) = \frac{1}{t_p}\int_0^{t_p} f(b\tau_m, E(t))dt, \tag{22}$$

where $t_p = t_p(b\tau)$ is the period. Here, we have written the environment E explicitly as a function of time t, but for simplicity we often drop time from our notations. When the environment

is at an equilibrium, then the population growth rate f described by (21) fully determines the long-term fitness of the mutant. Note that whether the resident environment is equilibrium or periodic is intentionally inexplicit in the notation for E. The reasoning behind this choice of notation is to avoid situations in which statements are made for certain types of environments that are absent for some trait values.

To find the value of invasion fitness numerically, we first solved the ecological attractors for the resident trait and checked whether there is bistability. Whenever a resident trait corresponds to two stable ecological attractors, these cases were treated separately. Invasion fitness in equilibrium environment can be solved directly by using (21), in which E is replaced by the corresponding equilibrium environment. In periodic environments, we solved (22) using the *NIntegrate* method of *Mathematica*®. The state of the resident environment $E(t)$ for each $t \in [0, t_p]$ was evaluated using the periodic orbit obtained by the Poincaré section, the details of which are found in Section 3.

By definition, every resident must have fitness equal to zero, as on average their abundances neither grow nor decline. Thus, every resident $b\tau$ satisfies $r_E(b\tau) = 0$. As the environment E consists of two components, then at most two coexisting prey types can simultaneously have zero fitness: a result known as the principle of competitive exclusion (MacArthur and Levins, 1964; Geritz et al., 1997). Thus, the environment sets the upper limit of diversity attainable through evolution. Note that while it is possible to find parameters for which two prey types coexist, long-term evolution may cause one of those prey types to go extinct.

Through repeated invasion and exclusion events, $b\tau$ evolves in the direction described by the fitness derivative,

$$D(b\tau) = \left[\frac{\partial r_E(b\tau_m)}{\partial (b\tau_m)}\right]_{b\tau_m = b\tau}, \tag{23}$$

which as with the invasion fitness, is evaluated at the ecological environment where the resident is present. The directional evolution comes to a halt when the fitness derivative vanishes, $D(b\tau^*) = 0$, and such a value $b\tau^*$ is called an evolutionary singularity. Furthermore, a singularity that is attainable through evolution is an evolutionary attractor. In this paper, all evolutionary singularities are also evolutionary attracting. Note that if an alternative ecological environment exists for the trait $b\tau = b\tau^*$, then this trait is unlikely to be an evolutionary attractor for the alternative environment. Also, note that when evolution drives $b\tau$ all the way down to zero, then generally the fitness derivative is negative at $b\tau = 0$. In such a case, the trait $b\tau = 0$ is an evolutionary attractor, but it is conceptually different from an evolutionary singularity. Whenever a need arises to distinguish between the ecological environments in which an evolutionary attractor is present, we write $b\tau^\bullet$ and $b\tau^\circ$, respectively, for equilibrium and periodic environments.

An evolutionary singularity is evolutionarily stable if it is uninvadable by any new mutant (Maynard Smith, 1982; Geritz et al., 1998). It follows that a singular trait $b\tau^*$ is evolutionarily stable if the invasion fitness is at a maximum,

$$\left[\frac{\partial^2 r_E(b\tau_m)}{\partial (b\tau_m)^2}\right]_{b\tau_m = b\tau = b\tau^*} < 0. \tag{24}$$

Throughout the numerical analysis, at most one evolutionary singularity existed for the branch of periodic attractors. Moreover, such singularities were always attracting and evolutionarily stable, providing no evidence for evolutionary branching. But since we are only able to obtain the periodic environment E numerically, excluding evolutionary branching altogether is difficult. Likewise, evidence is lacking for the existence of multiple singularities for the branch of periodic attractors. In a related model without cannibalism, Geritz and Gyllenberg (2014) came to similar conclusions.

Lower levels of timidity are always favoured by natural selection in equilibrium environments, as shown by Geritz and Gyllenberg (2014). Therefore, when bifurcations are absent for these environments, the evolutionary outcome is $b\tau^\bullet = 0$. On the other hand, when the equilibrium is unstable for $b\tau = 0$, then evolution by natural selection will cause Hopf bifurcation of the ecological environment. Recall that in our model, both sub- and supercritical Hopf bifurcations can occur. When the Hopf bifurcation is supercritical, there is a smooth transition between the equilibrium and periodic environments, and the direction of evolution remains unchanged. Later when the periodic environments have larger amplitude, evolution may attain a positive singularity $b\tau^\circ > 0$.

When the equilibrium undergoes a subcritical Hopf bifurcation, a discontinuous transition occurs between equilibrium and periodic environments. After passing subcritical bifurcation through evolution, the ecological environment settles on the alternative periodic attractor already present in the system. Such an attractor switch may also reverse the direction of evolution, which we call an evolutionary reversal. If such an evolutionary reversal occurs when switching from an equilibrium to a periodic attractor, it means that higher levels of timidity are now favoured by natural selection. Then, by tracing evolution along the branch of periodic attractors, either a singularity $b\tau^\circ$ is attained, or the evolution crosses the point of fold bifurcation. If the latter outcome occurs, the periodic environment disappears and an attractor switch causes the environment to settle on the equilibrium attractor. Such an attractor switch also causes an evolutionary reversal, whereupon selection favours lower levels of timidity. Eventually, the equilibrium environment disappears through the subcritical Hopf bifurcation, and the whole process repeats again. In other words, this process describes evolutionary cycling of the level of timidity.

A simple classification of qualitatively different evolutionary scenarios is constructed from two ingredients. The first depends on the existence of ecological attractors, and the second on the evolutionary dynamics along the ecological attractors. Assuming that at most one evolutionary attractor exists for each branch of ecological attractors, we find ten classes of evolutionary scenarios. These are denoted by Roman numerals I-X, and are catalogued in Table 2. Numerical analysis reveals that all of the evolutionary scenarios are possible. Fig. 4 shows a typical example of the parameter regions in the (α, β)-plane resulting in these scenarios. For each scenario, we have also provided an example of the evolutionary dynamics of $b\tau$ using pairwise invasibility plots for each ecological attractor. For information on how to read pairwise invasibility plots, see Geritz et al. (1998). In the following analysis, recall that the bifurcation regions of the ecological dynamics are illustrated in Fig. 3.

In scenario I, the ecological dynamics are described by bifurcation region A. The environment is always at an equilibrium, and timidity evolves all the way down to zero, $b\tau^\bullet = 0$.

In scenario II, the ecological dynamics are described by bifurcation region B. When the environment traces the branch of equilibrium attractors, evolution crosses a supercritical Hopf bifurcation, after which the environment is periodic. Then, while tracing the branch of periodic attractors, timidity evolves all the way down to zero, $b\tau^\circ = 0$. For example, when $\alpha = 0$ and $\beta = 4$, the supercritical Hopf bifurcation occurs at $b\tau^H = 0.1745$.

In scenario III, the ecological dynamics are described by bifurcation region B. When the environment traces the branch of equilibrium attractors, evolution crosses a supercritical Hopf bifurcation, after which the environment is periodic. Then, while tracing the branch of periodic attractors, timidity evolves to a positive singularity, $b\tau^\circ > 0$. For example, when $\alpha = 0$ and $\beta = 6$, the supercritical Hopf bifurcation occurs at $b\tau^H = 0.6298$, and the singularity is at $b\tau^\circ = 0.3864$.

In scenario IV, the ecological dynamics are described by bifurcation region C. When the environment traces the branch of equi-

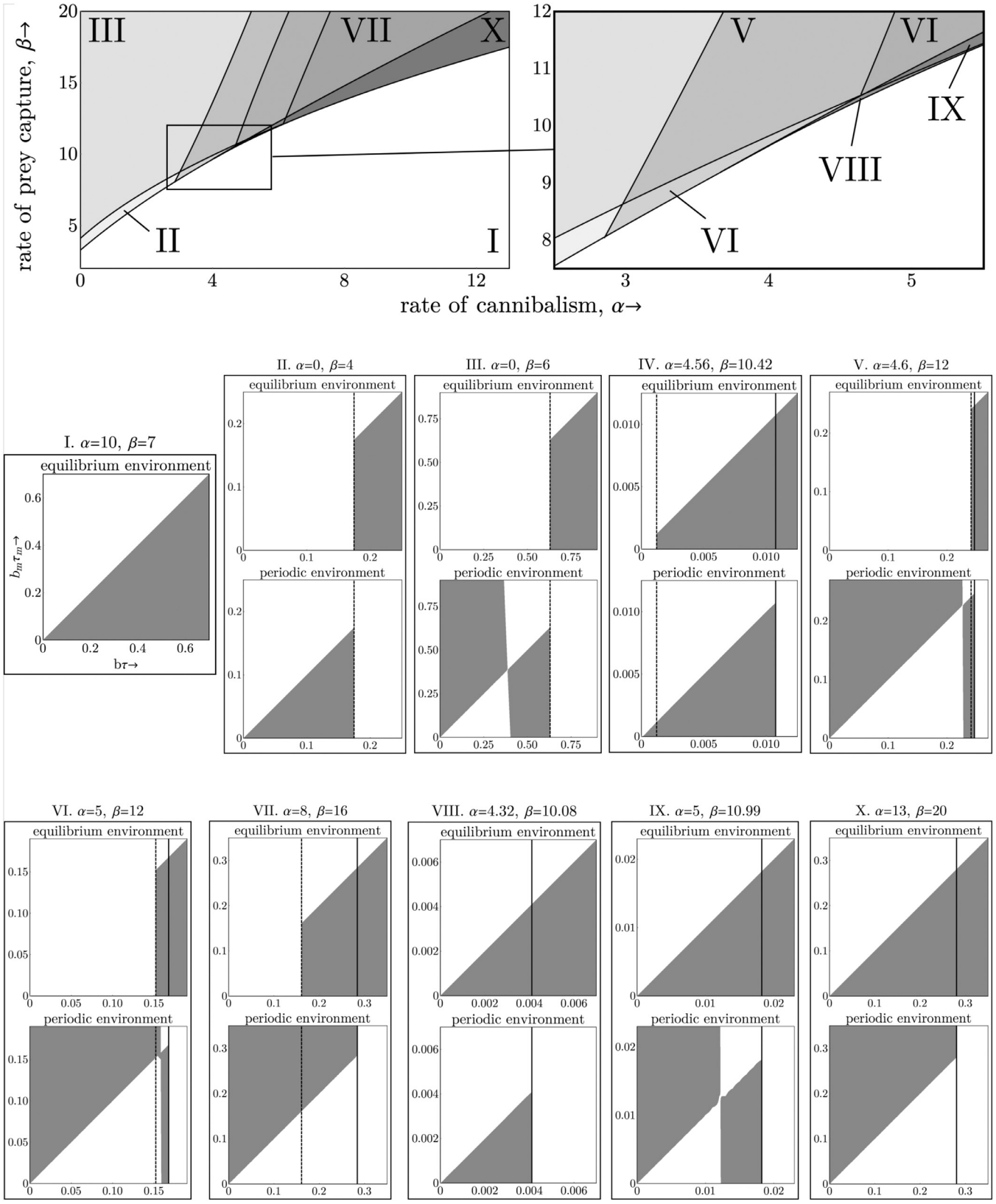

Fig. 4. Regions of qualitatively different evolutionary scenarios in the (α, β)-plane (*above*), and examples of pairwise invasibility plots (PIP) for each scenario (*below*). Table 2 provides detailed descriptions of these scenarios. In each PIP shaded regions depict the mutant traits that can invade the resident trait. Dashed and thick vertical lines indicate, respectively, Hopf and fold bifurcations. The parameters are the same as in Fig. 2.

Table 2
List of qualitatively different evolutionary scenarios. Evolutionary attractors corresponding to equilibrium and periodic environments are distinguished by $b\tau^{\bullet}$ and $b\tau^{\circ}$, respectively.

Evolutionary scenario	Bifurcation region	Bifurcations via evolution	Evolutionary reversals	Evolutionary attractors
I	A	none	no	$b\tau^{\bullet}=0$
II	B	supercritical Hopf	no	$b\tau^{\circ}=0$
III	B	supercritical Hopf	no	$b\tau^{\circ}>0$
IV	C	subcritical Hopf	no	$b\tau^{\circ}=0$
V	C	subcritical Hopf	no	$b\tau^{\circ}>0$
VI	C	subcritical Hopf	yes	$b\tau^{\circ}>0$
VII	C	subcritical Hopf and fold	yes	evolutionary cycle
VIII	D	none	no	$b\tau^{\bullet}=0$ and $b\tau^{\circ}=0$
IX	D	none	no	$b\tau^{\bullet}=0$ and $b\tau^{\circ}>0$
X	D	fold	yes	$b\tau^{\bullet}=0$

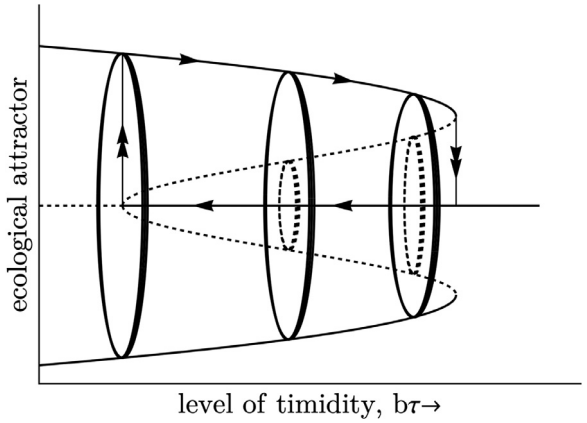

Fig. 5. Graphical illustration of an evolutionary cycle driven by ecological attractor switching.

librium attractors, evolution crosses a subcritical Hopf bifurcation and the environment switches to the periodic attractor. However, the direction of evolution is unchanged. Then, while tracing the branch of periodic attractors, timidity evolves all the way down to zero, $b\tau^{\circ}=0$. For example, when $\alpha=4.56$ and $\beta=10.42$, the subcritical Hopf and fold bifurcations occur at $b\tau_H=0.0012$ and $b\tau_F=0.0107$, respectively. Therefore, ecological bistability is present for $b\tau\in(0.0012, 0.0107)$.

In scenario V, the ecological dynamics are described by bifurcation region C. When the environment traces the branch of equilibrium attractors, evolution crosses a subcritical Hopf bifurcation and the environment switches to the periodic attractor. However, the direction of evolution is unchanged. Then, while the environment traces the branch of periodic attractors, timidity evolves to a positive singularity, $b\tau_H>b\tau^{\circ}>0$. For example, when $\alpha=4.6$ and $\beta=12$, the subcritical Hopf and fold bifurcations occur at $b\tau_H=0.2410$ and $b\tau_F=0.2467$, respectively, and the evolutionary singularity is at $b\tau^{\circ}=0.2266$. Therefore, ecological bistability is present for $b\tau\in(0.2410, 0.2467)$.

In scenario VI, the ecological dynamics are described by bifurcation region C. When the environment traces the branch of equilibrium attractors, evolution crosses a subcritical Hopf bifurcation and the environment switches to the periodic attractor. This attractor switch also causes an evolutionary reversal towards higher levels of timidity. Then, while the environment traces the branch of periodic attractors, timidity evolves to a positive singularity, $b\tau^{\circ}>b\tau_H$. For example, when $\alpha=5$ and $\beta=12$, the subcritical Hopf and fold bifurcations occur at $b\tau_H=0.1520$ and $b\tau_F=0.1676$, respectively, and the evolutionary singularity is at $b\tau^{\circ}=0.1582$. Therefore, ecological bistability is present for $b\tau\in(0.1520, 0.1676)$.

In scenario VII, the ecological dynamics are described by bifurcation region C. When the environment traces the branch of equilibrium attractors, evolution crosses a subcritical Hopf bifurcation and the environment switches to the periodic attractor. This attractor switch also causes an evolutionary reversal towards higher levels of timidity. Then, while the environment traces the branch of periodic attractors, evolution crosses a fold bifurcation and the environment switches back to the equilibrium attractor. This attractor switch also causes an evolutionary reversal towards lower levels of timidity, and then repeats the whole process. In other words, this scenario describes cyclic prey evolution. Since evolutionary singularities are absent, an evolutionary cycle is attained for any initial trait $b\tau$ and any ecological environment. For example, when $\alpha=8$ and $\beta=16$, the subcritical Hopf and fold bifurcations occur at $b\tau_H=0.1608$ and $b\tau_F=0.2839$, respectively, and ecological bistability is present for $b\tau\in(0.1608, 0.2839)$. During the evolutionary cycle in this example, the evolving trait $b\tau$ is bounded in the interval (0.1608, 0.2839).

In scenario VIII, the ecological dynamics are described by bifurcation region D. Whether the environment traces the branch of equilibrium or periodic attractors, timidity always evolves all the way down to zero. Thus, the evolutionary attractors are $b\tau^{\bullet}=0$ and $b\tau^{\circ}=0$, respectively, for equilibrium or periodic environments. Bifurcations are never encountered through evolution, and the ecological dynamics remain similar throughout the course of evolution. Therefore, the initial ecological state fully determines whether the environment traces the branch of equilibrium or periodic attractors. For example, when $\alpha=4.32$ and $\beta=10.08$, the fold bifurcation occurs at $b\tau_F=0.0041$, and ecological bistability is present for $b\tau\in[0, 0.0041)$.

In scenario IX, the ecological dynamics are described by bifurcation region D. When the environment traces the branch of equilibrium attractors, timidity evolves all the way down to zero, $b\tau^{\bullet}=0$. When the environment traces the branch of periodic attractors, timidity evolves to a positive singularity, $b\tau^{\circ}>0$. Bifurcations are never encountered through evolution, and the ecological dynamics remain similar throughout the course of evolution. For example, when $\alpha=5$ and $\beta=10.99$, the fold bifurcation occurs at $b\tau_F=0.0182$, and the evolutionary singularity for the branch of periodic attractors is at $b\tau^{\circ}=0.0122$. Therefore, ecological bistability is present for $b\tau\in[0, 0.0182)$.

In scenario X, the ecological dynamics are described by bifurcation region D. When the environment traces the branch of equilibrium attractors, timidity evolves all the way down to zero, $b\tau^{\bullet}=0$. When the environment traces the branch of periodic attractors, evolution crosses a fold bifurcation and the environment switches to the equilibrium attractor. This attractor switch also causes an evolutionary reversal towards lower levels of timidity. Thus, the evolutionary outcome is the same for any initial state, but the course of evolution may involve a detour towards higher levels of timidity. For example, when $\alpha=13$ and $\beta=20$, the fold bifurcation occurs at $b\tau_F=0.2802$ and ecological bistability is present for $b\tau\in[0, 0.2802)$.

Based on the data collected for Fig. 4, the prevalences of different evolutionary outcomes are as follows. Scenario I: 54.155%, scenario II: 0.848%, scenario III: 22.673%, scenario IV: 0.143%, scenario V: 5.164%, scenario VI: 4.432%, scenario VII: 7.625%, scenario VIII: 0.029%, scenario IX: 0.121%, and scenario X: 4.810%.

5. Discussion

In this paper, we investigated the evolution of timidity in a prey species whose predator has cannibalistic tendencies. The ecological model was derived from individual-level processes in the spirit of Geritz and Gyllenberg (2014), who investigated the same subject but without cannibalistic predators. We found that cannibalism induces ecological bistability between equilibrium and periodic attractors. We classified ten qualitatively different evolutionary scenarios, in which ecological bistability plays a central role. In particular, the analysis revealed that the end result can be an evolutionary cycle of the level of timidity, driven by ecological attractor switching and evolutionary reversals (scenario VII, 7.6% prevalence in Fig. 4). This evolutionary scenario falls under the ecogenetically-driven cycles in the classification of Khibnik and Kondrashov (1997).

For evolutionary cycling and evolutionary reversals to occur in our model (scenarios VI, VII, and X), two conditions must be satisfied on the ecological timescale. Firstly, periodic ecological environments are necessary for positive levels of timidity to be favoured by natural selection. Secondly, ecological bistability is necessary for attractor switching to occur. Fig. 5 illustrates the role of these ecological conditions in evolutionary cycling. The second condition follows from the fact that without ecological bistability, the level of timidity uniquely determines the direction of evolution. Admittedly, without ecological bistability, it may be possible to find cycles of evolutionary branching and extinction, in which a species branches into two types only to be later followed by a chance extinction of one of them (Kisdi et al., 2001; Dercole, 2003). Here we have found no evidence for evolutionary branching nor extinction, suggesting that the branching-extinction cycle is unlikely in our model.

We now ask which individual-level processes drive the aforementioned ecological conditions for evolutionary cycling and evolutionary reversals, and particularly, what are the roles of cannibalism and timidity in such outcomes? Could we relax some of the assumptions made on the basis of individual-level processes, such as non-negligible handling time per prey capture, while still satisfying these ecological conditions?

All evidence obtained here suggests that both cannibalism and timidity can only forestall the occurrence of periodic ecological attractors. Whenever a periodic attractor is present, increasing either cannibalism or timidity always causes it to disappear either through a supercritical Hopf or a fold bifurcation. This implies that if there are no periodic attractors in the absence of cannibalism and timidity, then equilibrium is always the only attractor.

It is well known that the ecological dynamics (15) and (16) with $b\tau = \alpha = h = 0$ can only have equilibrium attractors. Therefore, non-negligible handling time per prey capture is necessary for the existence of periodic attractors. When $h > 0$, we found that periodic attractors are easily obtained by increasing β. However, when β is set to a relatively large value, the populations at the periodic attractor go near to extinction and the model loses biological significance. When the parameters were as in Fig. 2 and $b\tau = \alpha = 0$, such problems arose at $\beta = 25$, where the minimum prey population at the attractor was less than 10^{-19}.

While we found that cannibalism seems to induce ecological bistability, understanding why this occurs is difficult. Part of the difficulty is because in our model, ecological bistability is always between equilibrium and periodic attractors. Since periodic attractors are rather difficult to deal with analytically, we were unable to perform a thorough investigation on the role of cannibalism in ecological bistability. Nevertheless, the numerical analysis suggests that ecological bistability is often induced by increasing cannibalism if, in the absence of cannibalism, the periodic attractor has a large amplitude. Curiously, cannibalism is known to induce ecological bistability in models of different nature, including models where the time and the population structure are both continuous (Claessen and de Roos, 2003), or where the time is discrete but the population structure is continuous (Cushing, 1991). In these models, ecological bistability typically occurs between multiple equilibrium states. In comparison, the present model assumes a discrete population structure and a continuous time.

In the present paper we have investigated only the evolution of the prey, but in nature the predator and the prey typically evolve together. For example, if the prey evolves to favour high levels of timidity, it effectively reduces the food availability for the predator. Thus, prey evolution exerts selective pressure on the predator, which must now find a way to compensate for the lack of food. We envision that cannibalism could then emerge as the predator's evolutionary response. However, we have reason to believe that in reality, cannibalism has various direct trade-offs, such as non-negligible handling time for cannibalism or decreased rate of prey capture. Thus, cannibalism may evolve only when the benefits exceed the costs, which depend both on the environmental conditions and the trade-off that cannibalism poses on other individual-level processes.

As natural selection acts only for the benefit of the individual, evolution of cannibalism may have a decreasing effect on the predator population. When cannibalism is harmful for the predator population, but they become voracious cannibals through evolution, then fewer prey are captured. Consequently, lower levels of timidity become favourable, reversing the direction of prey evolution. Eventually, the benefits of cannibalism are lessened by increased prey availability, whereupon natural selection favours less cannibalistic predators. Such coevolutionary dynamics between the predator and the prey species may lead to a purely genetically-driven evolutionary cycle without switching between ecological attractors (Dieckmann et al., 1995).

The analysis conducted here shows that model derivation from individual-level processes is essential in making predictions concerning both the ecological and the evolutionary outcomes. We have shown that a single trait can correspond to multiple ecological attractors, and these attractors can disappear as a consequence of evolution. Switching between alternative attractors is a likely evolutionary consequence of ecological bistability, and it can also bring about evolutionary reversals and evolutionary cycling. Fortunately, the necessary techniques for evolutionary analysis with ecological bistability are readily implemented in the framework of adaptive dynamics. Most often the difficulties in our research had to do with numerical analysis, and less with model derivation or the theoretical framework.

Acknowlgedgments

This research was funded by the Academy of Finland, Centre of Excellence in Analysis and Dynamics Research.

Appendix A

On the separation of ecological timescales

The dynamical system of the interactions between all five individual states is given by

$$\frac{dx_i^F}{dt} = -b_i x_i^F y + \frac{1}{\tau_i} x_i^H - \beta x_i^F y^S$$

$$+x_i^F G\Big(\sum_j x_j^F\Big) - \mu x_i^F, \tag{A.1}$$

$$\frac{dx_i^H}{dt} = b_i x_i^F y - \frac{1}{\tau_i} x_i^H - \mu x_i^H, \tag{A.2}$$

$$\frac{dy^S}{dt} = -\beta y^S \sum_j x_j^F + \frac{1}{h} y^H - \delta y^S + \frac{1}{T} z, \tag{A.3}$$

$$\frac{dy^H}{dt} = \beta y^S \sum_j x_j^F - \frac{1}{h} y^H - \delta y^H, \tag{A.4}$$

$$\frac{dz}{dt} = (\lambda - 1)\alpha y^S z + \gamma \beta y^S \sum_j x_j^F - \sigma z - \frac{1}{T} z. \tag{A.5}$$

We now separate the above dynamics into three separate timescales. Let $\varepsilon > 0$ be a small and dimensionless scaling parameter, and assume the following scalings for the model parameters: $b = \varepsilon^{-3} b_0$, $\alpha = \varepsilon^{-2}\alpha_0$, $\beta = \varepsilon^{-1}\beta_0$, $\sigma = \varepsilon^{-1}\sigma_0$, $T = \varepsilon^{-1} T_0$, $x = \varepsilon^{-1} x_{0'}$, $y = \varepsilon y_0$, $\tau = \varepsilon^2 \tau_0$, $h = \varepsilon^2 h_0$, and $G(\sum_j x_j^F) = G_0(\varepsilon \sum_j x_j^F)$. Next, rewrite the above system using these scaled parameters, and the equations for the total prey and adult predator populations, $x_i = x_i^F + x_i^H$ and $y = y^S + y^H$. For convenience, we also drop the subindex zero from these scaled parameters, which results in

$$\begin{aligned}\varepsilon^2 \frac{dx_i^F}{dt} &= -b_i x_i^F y + \frac{1}{\tau_i} x_i^H - \varepsilon^2 \beta x_i^F y^S \\ &\quad + \varepsilon^2 x_i^F G\Big(\sum_j x_j^F\Big) - \varepsilon^2 \mu x_i^F,\end{aligned} \tag{A.6}$$

$$\frac{dx_i}{dt} = x_i^F G\Big(\sum_j x_j^F\Big) - \mu x_i - \beta x_i^F y^S, \tag{A.7}$$

$$\frac{dy}{dt} = \frac{1}{T} z - \delta y, \tag{A.8}$$

$$\varepsilon^2 \frac{dy^S}{dt} = -\beta y^S \sum_j x_j^F + \frac{1}{h} y^H - \varepsilon^2 \delta y^S + \frac{\varepsilon^2}{T} z, \tag{A.9}$$

$$\varepsilon \frac{dz}{dt} = (\lambda - 1)\alpha y^S z + \gamma \beta y^S \sum_j x_j^F - \sigma z - \frac{\varepsilon^2}{T} z. \tag{A.10}$$

To investigate the above dynamics on the short timescale, we introduce a scaled time $t^{**} := \varepsilon^{-2} t$, and let $\varepsilon \to 0$. Then, the dynamics are given by

$$\frac{dx_i^F}{dt^{**}} = -b_i x_i^F y + \frac{1}{\tau_i} x_i^H, \tag{A.11}$$

$$\frac{dy^S}{dt^{**}} = -\beta y^S \sum_j x_j^F + \frac{1}{h} y^H, \tag{A.12}$$

which are equivalent to (3) and (4), and where the variables x, y, and z are constants on this timescale. Next, assuming that the short timescale dynamics have attained a quasi-steady state, we investigate the dynamics (A.6)–(A.10) on the intermediate timescale. Rewrite these dynamics using the quasi-steady states (5) and (6) for the short timescale, and introduce a scaled time $t^* := \varepsilon^{-1} t$. Then, let $\varepsilon \to 0$, which results in

$$\frac{dz}{dt^*} = \gamma \beta y^S \sum_j x_j^F + \alpha \lambda y^S z - \alpha y^S z - \sigma z, \tag{A.13}$$

which is equivalent to (7), and where x_i and y are constants in this intermediate timescale.

For an alternative scaling with only two timescales, assume that y, z, τ, and h are of order ε; β and σ are of order ε^{-1}; and that α and b are of order ε^{-2}. Now, when the dynamics of both the state-transitions and the juvenile population dynamics are studied on the $t^* := \varepsilon^{-1} t$ timescale, we find exactly the same quasi-equilibria as before. Thus, the only differences are in the biological interpretation; in the case with two timescales we assumed that the adult and the juvenile predator population numbers are on the same scale, and predator maturation time is much shorter.

Appendix B

On the existence and uniqueness of an interior equilibrium

Any interior equilibrium corresponds to an intersection between isoclines. At the prey isocline we have $\dot{x} = 0$, which we write in terms of x^F,

$$\tilde{y}_1 = \frac{(G(x^F) - \mu)(1 + \beta h x^F)}{\beta + \mu b \tau (1 + \beta h x^F)}. \tag{B.1}$$

The prey isocline is positive for $x^F < x_0$, and has unique root at $x^F = x_0$. The second derivative of the prey isocline with respect to x^F is given by

$$\begin{aligned}\tilde{y}_1'' = \Big[&2\beta^2 h(b\tau\beta h\mu(\mu - G(x^F)) \\ &+ (\beta + b\tau\mu(1 + \beta h x^F))G'(x^F)) \\ &+ (1 + \beta h x^F)(\beta + b\tau\mu(1 + \beta h x^F))^2 G''(x^F)\Big] \\ &/(\beta + b\tau\mu(1 + \beta h x^F))^3,\end{aligned} \tag{B.2}$$

which is concave if and only if

$$\begin{aligned}G''(x^F) < \; &2\beta^2 h(b\tau\beta h\mu(G(x^F) - \mu) \\ &- (\beta + b\tau\mu(1 + \beta h x^F))G'(x^F).\end{aligned} \tag{B.3}$$

In particular, for any G such that $G'' \le 0$ the above condition holds. Similarly, we write the predator isocline in terms of x^F,

$$\tilde{y}_2 = \frac{\beta(\gamma - \delta\sigma h T)x^F - \delta\sigma T}{\alpha\delta T(1 - \lambda)}. \tag{B.4}$$

The predator isocline increases monotonically in x^F for $\gamma > \delta\sigma h T$ and $\lambda < 1$, and positive for $\beta > \delta\sigma T/(x^F(\gamma - \delta\sigma h T))$. Both of these conditions are satisfied whenever the predator can invade the environment where only the prey is present. By continuity $\tilde{y}_2$ is also positive for some $x^F < x_0$. This implies the existence of $x_1 < x_0$ at which the isoclines intersect, and where x_1 satisfies

$$\frac{(G(x_1) - \mu)(1 + \beta h x_1)}{\beta + \mu b \tau (1 + \beta h x_1)} = \frac{\beta(\gamma - \delta\sigma h T)x_1 - \delta\sigma T}{\alpha\delta T(1 - \lambda)}. \tag{B.5}$$

In other words, an interior equilibrium exists. If also (B.3) holds, then the uniqueness follows from the concavity of the prey isocline and the monotonicity of the predator isocline.

Appendix C

On the stability of the interior equilibrium

Let $\operatorname{tr} J$ and $\det J$ denote the trace and the determinant of the 2×2 Jacobian matrix J of (15) and (16) evaluated at the interior equilibrium $(\bar{x}, \bar{y}) = (x_1(1 + b\tau\bar{y}), \bar{y})$. We show that the equilibrium can switch stability only through a Hopf bifurcation. First, we show that $\det J > 0$ for all $b\tau$ and α. Then, we show that for all $b\tau$, at most one α_1 exists for which $\operatorname{tr} J = 0$, and similarly, for all α, at most one $b\tau_1$ exists for which $\operatorname{tr} J = 0$. By the Routh-Hurwitz criteria, such values α_1 and $b\tau_1$ correspond to a Hopf bifurcation.

The determinant of J is given by

$$\det J = \gamma\beta\bar{y}x_1\Big[\alpha(1 - \lambda)\bar{y}(2b\tau\mu(1 + \beta h x_1)^2 + \beta(2 + \beta h x_1))$$

$$+(1+\beta h x_1)\{\sigma(\beta(1+b\tau h\mu x_1)+b\tau\mu) + \alpha(1-\lambda)\mu(1+\beta h x_1)\}+\alpha G(x_1)(\lambda-1)(1+\beta h x_1)^2 +\alpha(\lambda-1)x_1G'(x_1)(1+\beta h x_1)^2\Big]/ \Big[T(1+b\tau\bar{y})(1+\beta h x_1)^2(\sigma(1+\beta h x_1)+\alpha\bar{y}(1-\lambda))^2\Big]. \tag{C.1}$$

The sign of det J is given by the numerator in the above equation. Rewriting the numerator of det J in terms of $b\tau$ gives a linear equation, with positive coefficient

$$\gamma\mu\beta x_1\bar{y}(1+\beta h x_1)^2(2\alpha\bar{y}(1-\lambda)+\sigma), \tag{C.2}$$

and so the numerator of det J is minimised at $b\tau=0$. Substituting $b\tau=0$ and $\mu=G(\bar{x})-\beta\bar{y}/(1+\beta h\bar{x})$ into the numerator of det J results in

$$\alpha(\lambda-1)\bar{x}G'(\bar{x})(1+\beta h\bar{x})^2+\beta(\sigma(1+\beta h\bar{x})+\alpha\bar{y}(1-\lambda)), \tag{C.3}$$

which is positive for all α. Therefore, det J is strictly positive for all $b\tau$. Similarly, rewriting the numerator of det J in terms of α gives a linear equation, with coefficient

$$\gamma\beta(\lambda-1)x_1\bar{y}\Big[G(x_1)(1+\beta h x_1)^2-\beta\bar{y}(2+\beta h x_1) +(1+\beta h x_1)^2(x_1G'(x_1)-(1+2b\tau\bar{y})\mu)\Big]. \tag{C.4}$$

Then, upon substituting $G(x_1)=\mu(1+b\tau\bar{y})+\beta\bar{y}/(1+\beta h x_1)$, the above coefficient is clearly positive. The numerator of det J in terms of α is then minimised at $\alpha=0$, and has the clearly positive value

$$\gamma\beta\sigma x_1\bar{y}(1+\beta h x_1)(\beta+b\tau\mu+b\tau\beta h\mu x_1). \tag{C.5}$$

We have now shown that det J is positive for all $b\tau$ and α.

The trace of the Jacobian matrix J is given by

$$\mathrm{tr}J=\frac{1}{1+b\tau\bar{y}}\Big[x_1G'(x_1)+\frac{\beta\bar{y}}{1+\beta h x_1}-\frac{\beta\bar{y}}{(1+\beta h x_1)^2} +\frac{\gamma\beta x_1\bar{y}(\alpha(\lambda-1)(1+2b\tau\bar{y})-b\tau\sigma)}{T(\alpha(\lambda-1)\bar{y}-\sigma(1+\beta h x_1))^2}\Big]. \tag{C.6}$$

To prove the claim, we shall show that the sign of tr J can change at most once in $b\tau$ and α. The derivative of tr J with respect to α is given by

$$\frac{\partial\mathrm{tr}J}{\partial\alpha}=\gamma\beta(1-\lambda)x_1\bar{y}\Big[\beta h\sigma x_1(1+2b\tau\bar{y}) +\alpha(\lambda-1)\bar{y}(1+2b\tau\bar{y})+\sigma\Big] /\Big[T(1+b\tau\bar{y})(\alpha(\lambda-1)\bar{y}-\sigma(1+\beta h x_1))^3\Big], \tag{C.7}$$

and vanishes at the positive value

$$\alpha_2=\frac{\sigma(1+\beta h x_1(1+2b\tau\bar{y}))}{(1-\lambda)(1+2b\tau\bar{y})\bar{y}}. \tag{C.8}$$

Moreover, since the derivative $\partial\mathrm{tr}J/\partial\alpha$ is negative at $\alpha=0$, then by continuity it is negative for all $\alpha<\alpha_2$, and positive for $\alpha>\alpha_2$. Next, observe that at the equilibrium

$$\bar{y}=\frac{\gamma\beta x_1-T\delta\sigma(1+\beta h x_1)}{\alpha T\delta(1-\delta)}, \tag{C.9}$$

and so $\bar{y}$ vanishes as $\alpha\to\infty$. Consequently, tr $J\to x_0G'(x_0)<0$. Now since $\partial\mathrm{tr}J/\partial\alpha$ vanishes only once and is initially negative, then tr J can change sign at most once in α. That is, whenever tr $J>0$ holds at $\alpha=0$, there exists unique $\alpha_1>0$ at which tr $J=0$. But if tr $J<0$ holds at $\alpha=0$, the trace remains negative for all $\alpha>0$.

Finally, we show that tr $J=0$ for at most one $b\tau=b\tau_1$. Since the term $1/(1+b\tau\bar{y})$ is strictly positive, it is sufficient to show the claim for tr J without that term. This results in a linear equation in $b\tau$, with coefficient

$$\frac{\gamma\beta x_1\bar{y}(2\alpha(\lambda-1)\bar{y}-\sigma)}{T(\beta h\sigma x_1+\alpha\bar{y}(1-\lambda)+\sigma)^2}, \tag{C.10}$$

which is clearly negative. Therefore, tr J is decreasing in $b\tau$ and can change sign at most once.

References

Abrams, P., Matsuda, H., 1997. Fitness minimization and dynamic instability as a consequence of predator-prey coevolution. Evolut. Ecol. 11 (1), 1–20. doi:10.1023/A:1018445517101.

Beddington, J., 1975. Mutual interference between parasites or predators and its effect on searching efficiency. J. Animal Ecol. 44 (1), 331–340. doi:10.2307/3866.

van den Bosch, F., de Roos, A., Gabriel, W., 1988. Cannibalism as a life boat mechanism. J. Math. Biol. 26, 619–633. doi:10.1007/BF00276144.

Claessen, D., de Roos, A., 2003. Bistability in a size-structured population model of cannibalistic fish - a continuation study. Theoret. Popul. Biol. 64 (1), 49–65. doi:10.1016/S0040-5809(03)00042-X.

Cushing, J., 1991. A simple model of cannibalism. Math. Biosci. 107 (1), 47–71. doi:10.1016/0025-5564(91)90071-P.

DeAngelis, D., Goldstein, R., O'Neill, R., 1975. A model for trophic interaction. Ecology 56 (4), 881–892. doi:10.2307/1936298.

Decaestecker, E., Gaba, S., Raeymaekers, J., Stoks, R., van Kerckhoven, L., Ebert, D., de Meester, L., 2007. Host-parasite 'Red Queen' dynamics archived in pond sediment. Nature 450, 870–873. doi:10.1038/nature06291.

Dercole, F., 2003. Remarks on branching-extinction evolutionary cycles. J. Math. Biol. 47 (6), 569–580. doi:10.1007/s00285-003-0236-4.

Dercole, F., Ferrière, R., Rinaldi, S., 2002. Ecological bistability and evolutionary reversals under asymmetrical competition. Evolution 56 (6), 1081–1090. doi:10.1111/j.0014-3820.2002.tb01422.x.

Dercole, F., Rinaldi, S., 2002. Evolution of cannibalistic traits: scenarios derived from adaptive dynamics. Theor. Popul. Biol. 62 (4), 365–374. doi:10.1016/S0040-5809(02)00008-4.

Dieckmann, U., Marrow, P., Law, R., 1995. Evolutionary cycling in predator-prey interactions: population dynamics and the Red Queen. J. Theoret. Biol. 176 (1), 91–102. doi:10.1006/jtbi.1995.0179.

Doebeli, M., Ruxton, G., 1997. Evolution of dispersal rates in metapopulation models: branching and cyclic dynamics in phenotype space. Evolution 51 (6), 1730–1741. doi:10.2307/2410996.

Edgar, W., 1969. Prey and predators of the wolf spider Lycosa Lugubris. J. Zool. 159 (4), 405–411. doi:10.1111/j.1469-7998.1969.tb03897.x.

Fox, L., 1975. Cannibalism in natural populations. Ann. Rev. Ecol. Syst. 6 (1), 87–106. doi:10.1146/annurev.es.06.110175.000511.

Geritz, S., Gyllenberg, M., 2012. A mechanistic derivation of the Deangelis-Beddington functional response. J. Theor. Biol. 314, 106–108. doi:10.1016/j.jtbi.2012.08.030.

Geritz, S., Gyllenberg, M., 2014. The DeAngelis-Beddington functional response and the evolution of timidity of the prey. J. Theor. Biol. 359, 37–44. doi:10.1016/j.jtbi.2014.05.015.

Geritz, S., Gyllenberg, M., Jacobs, F., Parvinen, K., 2002. Invasion dynamics and attractor inheritance. J. Math. Biol. 44 (6), 548–560. doi:10.1007/s002850100136.

Geritz, S., Kisdi, É., Meszéna, G., Metz, J., 1998. Evolutionarily singular strategies and the adaptive growth and branching of the evolutionary tree. Evolut. Ecol. 12 (1), 35–57. doi:10.1023/A:1006554906681.

Geritz, S., Metz, J., Kisdi, É., Meszéna, G., 1997. Dynamics of adaptation and evolutionary branching. Phys. Rev. Lett. 78 (10), 2024–2027. doi:10.1103/PhysRevLett.78.2024.

Hauert, C., de Monte, S., Hofbauer, J., Sigmund, K., 2002. Volunteering as Red Queen mechanism for cooperation in public goods games. Science 296 (5570), 1129–1132. doi:10.1126/science.1070582.

Hjelm, J., Persson, L., Christensen, B., 2000. Growth, morphological variation and ontogenetic niche shifts in perch (Perca fluviatilis) in relation to resource availability. Oecologia 122 (2), 190–199. doi:10.1007/PL00008846.

Hui, C., Minoarivelo, H., Landi, P., 2018. Modelling coevolution in ecological networks with adaptive dynamics. Math. Methods Appl. Sci. 41 (18), 8407–8422. doi:10.1002/mma.4612.

Khibnik, A., Kondrashov, A., 1997. Three mechanisms of Red Queen dynamics. Proc. R. Soc. B Biol. Sci. 264 (1384), 1049–1056. doi:10.1098/rspb.1997.0145.

Kisdi, É., Jacobs, F., Geritz, S., 2001. Red Queen evolution by cycles of evolutionary branching and extinction. Selection 2 (1), 161–176. doi:10.1556/Select.2.2001.1-2.12.

Kuznetsov, Y., 1998. Elements of Applied Bifurcation Theory, 2nd ed. Springer, New York doi:10.1007/b98848.

Law, R., Marrow, P., Dieckmann, U., 1997. On evolution under asymmetric competition. Evolut. Ecol. 11 (4), 485–501. doi:10.1023/A:1018441108982.

MacArthur, R., Levins, R., 1964. Competition, habitat selection, and character displacement in a patchy environment. Proc. Natl. Acad. Sci. USA 51 (6), 1207–1210. doi:10.1073/pnas.51.6.1207.

Matsuda, H., Abrams, P., 1994. Timid consumers: self-extinction due to adaptive change in foraging and anti-predator effort. Theor. Popul. Biol. 45 (1), 76–91. doi:10.1006/tpbi.1994.1004.

May, R., 1977. Thresholds and breakpoints in ecosystems with a multiplicity of stable states. Nature 269, 471–477. doi:10.1038/269471a0.

Maynard Smith, J., 1982. Evolution and the Theory of Games. Cambridge University Press, Cambridge doi:10.2277/0521288843.

Polis, G., 1981. The evolution and dynamics of intraspecific predation. Ann. Rev. Ecol. Syst. 12, 225–251. doi:10.1146/annurev.es.12.110181.001301.

Popova, O., Sytina, L., 1977. Food and feeding relations of eurasian perch (perca fluviatilis) and pikeperch (stizostedion lucioperca) in various waters of the USSR. J. Fisher. Res. Board Canada 34 (10), 1559–1570. doi:10.1139/f77-219.

Rietkerk, M., Dekker, S., de Ruiter, P., van de Koppel, J., 2004. Self-organized patch-

iness and catastrophic shifts in ecosystems. Science 305 (5692), 1926–1929. doi:10.1126/science.1101867.

Rosenzweig, M., MacArthur, R., 1963. Graphical representation and stability conditions of predator-prey interactions. Am. Natural. 97 (895), 209–223. doi:10.1086/282272.

Rueffler, C., Egas, M., Metz, J., 2006. Evolutionary predictions should be based on individual-level traits. Am. Natural. 168 (5), E148–E162. doi:10.1086/508618.

Scheffer, M., Carpenter, S., Foley, J., Folke, C., Walker, B., 2001. Catastrophic shifts in ecosystems. Nature 413, 591–596. doi:10.1038/35098000.

Vitale, C., Kisdi, É., 2018. Evolutionary suicide of prey: Matsuda and Abrams' model revisited. Bull. Math. Biol. doi:10.1007/s11538-018-0472-9.

Yom-Tov, Y., 1974. The effect of food and predation on breeding density and success, clutch size and laying date of the crow (Corvus Corone L.). J. Animal Ecol. 43 (2), 479–498. doi:10.2307/3378.